2023 IEEE International Conference on Next Generation Electronics (NEleX 2023)

Faithful Transfer of 3D Propagation Characteristics of Deterministic and Random Optical Fields to Coded Aperture Imaging Systems Using Lucy-Richardson-Rosen Algorithm

Agnes Pristy Ignatius Xavier
Institute of Physics, University of Tartu, Estonia.
School of Electrical and Computer Engineering, Ben Gurion University of the Negev, Israel.
agnes.pristy.ignatius.xavier@ut.ee

Francis Gracy Arockiaraj
Institute of Physics, University of Tartu, Estonia.
School of Electrical and Computer Engineering, Ben Gurion University of the Negev, Israel.
francis.gracy.arockiaraj@ut.ee

Shivasubramanian Gopinath
Institute of Physics, University of Tartu Estonia.
shivasubramanian.gopinath@ut.ee

Aravind Simon John Francis Rajeswary
Institute of Physics, University of Tartu Estonia.
aravind@ut.ee

Andra Naresh Kumar Reddy
Laboratory of Nonlinear Optics, University of Latvia, 1004 Riga, Latvia.
naresh.andra@lu.lv

Rashid A. Ganeev
Laboratory of Nonlinear Optics, University of Latvia, 1004 Riga, Latvia.
Tashkent Institute of Irrigation and Agricultural Mechanization Engineers, National Research University, Tashkent100000, Uzbekistan.
Department of Physics and Astronomy, Chirchik State Pedagogical University, Chirchik 111700, Uzbekistan.
rashid.ganeev@lu.lv

M. Scott Arockia Singh
Dr. Jeyasekharan Hospital Nagercoil 629003, Tamil Nadu, India.
Dr. Scott's Laser and Piles Fistula Center, Nagercoil 629201, Tamil Nadu, India
leandrascott@gmail.com

S.D. Milling Tania
Department of Orthodontics, Rajas Dental College, and Hospital, Tirunelveli 627105, Tamil Nadu, India.
Darshan Dental and Orthodontic Clinic, Kanyakumari 629401, Tamil Nadu, India.
drtania_d@yahoo.co.in

Vijayakumar Anand
Institute of Physics, University of Tartu, Estonia.
Optical Sciences Center and ARC Training Centre in Surface Engineering for Advanced Materials (SEAM),
School of Science, Computing and Engineering Technologies, Swinburne University of Technology,
Hawthorn, Melbourne, VIC 3122, Australia.
vijayakumar.anand@ut.ee

***Abstract*— Engineering the complex amplitude and polarization of light is essential for various applications. In this direction, many deterministic and random optical beams such as Airy Bessel, and self-rotating beams were developed. While the above beams satisfied the requirements for the targeted applications, they are not suitable for imaging applications in spite of the valuable axial characteristics they possess, as they are not effective object-image mapping elements. Consequently, when exotic beams were implemented for direct imaging, only a distorted image was obtained. However, the scenario is different in coded aperture imaging (CAI) methods, where the imaging mode is indirect, consisting of optical recording and computational image recovery. Therefore, the point spread function (PSF) in CAI is not the recorded intensity distribution but the reconstructed intensity distribution. By employing a suitable computational reconstruction method, it is possible to convert the recorded intensity distribution into a Delta-like function. In this study, Lucy-Richardson-Rosen algorithm has been implemented as a generalized image recovery method for a wide range of optical beams, and the performance is validated in both simulation and optical experiments.**

Keywords*— *computational imaging, coded aperture imaging; Lucy–Richardson–Rosen algorithm; digital holography; microscopy; diffractive optics.

I. Introduction

Beam shaping is a well-known technique used for shaping either amplitude, phase, or polarization or all of the above of the optical beams [1]. Some of the widely generated optical beams are Gaussian beams, Laguerre-Gaussian beams, Airy beams, self-rotating beams, Bessel beams, each of which can be tailored to exhibit specific beam shaping attributes to suit various applications [2]. For instance, Gaussian beams, characterized by their bell-shaped intensity profiles, find

This research was funded by European Union's Horizon 2020 research and innovation pro-gramme grant agreement No. 857627 (CIPHR).

979-8-3503-1908-8/23/$31.00 ©2023 IEEE

2023 International Conference on Next Generation Electronics (NEleX) | 979-8-3503-1908-8/23/$31.00 ©2023 IEEE | DOI: 10.1109/NELEX59773.2023.10421020

common use in optical trapping applications. Laguerre-Gaussian beams, featuring helical phase fronts and doughnut-like intensity profiles, are instrumental in optical trapping and optical communication [2]. Airy beams, known for their curved trajectory and self-healing properties, serve multiple purposes such as imaging through occlusion, whereas self-rotating beams, which exhibit intensity profile rotation during free-space propagation, are applied in optical communication. Finally, Bessel beams, showcasing a central bright spot surrounded by concentric rings, are ideal for optical trapping. Historically, beam shaping with these exotic beams was reserved for spatially coherent light sources, but some recent studies demonstrate that such beams can also be generated by spatially incoherent light sources [2]. These exotic optical beams are unique, designed for specific applications. Therefore, they are not ideal for regular imaging due to their unusual intensity patterns which are not like a focal point. To achieve the imaging application with exotic beams, it is necessary to do point-to-point mapping, which is like imaging with a simple lens when the imaging condition is satisfied. In this study, we consider only linear, shift-invariant systems. The imaging system consists of three components: object, optical modulator, and sensor. The point-to-point mapping can be done in the indirect imaging concept, with two steps as supposed to a single step in direct imaging concept. The two steps of the imaging process are namely optical recording and numerical image recovery. The indirect imaging process consists of a calibration process where the point spread function library is recorded once. After calibration, in the first step, an object is placed exactly at the same location as the pinhole and a single camera shot of the object intensity is captured. In the second step, the object intensity is processed with the PSF to reconstruct 2D spatial information of the object. The previous research on this topic began from coded aperture imaging (CAI) with an aim to create imaging technologies for non-visible electromagnetic regions, like X-rays and Gamma rays, where manufacturing lenses for such wavelengths was challenging [3]. In the first versions of CAI, a scattering type mask was used. This method was effective for 2D spatial and spectral imaging, but it couldn't capture 3D information. A significant breakthrough emerged with interferenceless coded aperture correlation holography (I-COACH), which bridged holography and CAI [4]. I-COACH employed quasi-random phase masks to record a library of PSFs for various axial positions instead of a single axial location as in previous studies. When the PSF library was processed with the object intensity pattern, 3D information of the object was reconstructed, effectively fusing incoherent holography with CAI. Subsequent research delved into optimizing phase masks and developing novel computational reconstruction methods to enhance the signal-to-noise ratio (SNR) [4]. There are different computational reconstruction methods that were used to retrieve the object information like matched filter, phase–only filter, Weiner filter, etc [4]. In 2017, a new novel reconstruction method called non–linear reconstruction (NLR) algorithm was introduced whose performance was effectively better than other methods [4]. NLR was experimented with both deterministic and random optical fields for 2D imaging, and the results showed promise [5]. In all the previous studies [4], there is a compatible modulation function - reconstruction method pair such as NLR and scattering mask and LRA and lens. The performances of LRA for a scattering mask and NLR for a lens are not optimal. Developing a universal reconstruction method for all types of modulation functions is highly desirable in order to extend dynamic 3D imaging to masks with unique and interesting characteristics. lately, a new image recovery method called Lucy–Richardson–Rosen algorithm (LR^{2}A) was developed by integrating Lucy–Richardson algorithm (LRA) with NLR [6]. LR^{2}A demonstrated superior performance compared to LRA and NLR in multiple studies [2,6]. The main motivation of this study is to investigate LR^{2}A as a universal reconstruction technique for different types of optical fields, to faithfully transfer the characteristics of these beams for 3D imaging applications.

II. Methodology

The optical configuration of indirect imaging using exotic beams and LR^{2}A is shown in Fig. 1. Light originating from an object impinges upon a phase mask, and the resultant modulated light is captured by an image sensor. The pre-recorded point spread functions (PSFs) serve as the reconstruction functions, enabling the extraction of 3D object information from LR^{2}A. Some interesting phase masks such as axicon, spiral axicon, diffractive lens and spiral lens, their PSFs and object intensities for a 'gift box' object and the reconstructions using LR^{2}A are shown in Fig. 1. The imaging process can be expressed as follows. The object intensity recorded for an object O is given as $I = O \otimes PSF$, where '$\otimes$' is a 2D convolutional operator. The image reconstruction is given as $I_R = I \circledcirc^{n}_{\alpha,\beta} PSF$, where '$\circledcirc^{n}_{\alpha,\beta}$' represents the LR^{2}A operator, where α and β are tuned between -1 and 1 to optimize the magnitudes of the spectrum and n is the number of iterations. In LR^{2}A, there are two domains, namely, the sensor domain and the object domain. The information in the sensor domain and an initial guess solution of O are validated using the fundamental equation $I = O \otimes PSF$, and the measured discrepancy is transferred to the object domain to improve the previous solution of O. This process is iterated until the fundamental equation is satisfied. The steps of LR^{2}A are discussed next. Step 1: An initial guess R^1 of the object O is made, which is usually the object intensity I in LRA as it was widely used on blurred images; the same has been adapted to LR^{2}A. However, the initial guess can be any matrix; the closer it is to the solution, the faster the convergence. Step 2: The guessed solution is convolved with the PSF to obtain the object intensity I'. Step 3: The ratio between I and I' is calculated. Step 4: This ratio in the sensor domain is transferred to the object domain using a correlation operation between the PSF and the ratio in LRA, which is replaced by NLR. Consequently, the discrepancy in the object domain is estimated with a high SNR. Step 5: This is used to improve the previous solution R^1 to R^2, which is closer to O. The steps 1 to 5 are iterated, and in every iteration, the previous solution is replaced by a new one until the solution converges to the ideal solution O. The values of α, β and n are tuned to obtain an optimal solution set by a suitable figure of merit such as structural similarity index or root mean squared error. The main difference between LRA and LR^{2}A is the replacement of regular correlation or matched filter by NLR. There are many studies, including, where NLR has been compared with matched filter, and a significant improvement in SNR has been demonstrated for NLR. This improvement which occurs in step – 4, impacts the entire algorithm resulting in a faster convergence and improved estimation compared to LRA. Through this process, it is possible to create a calibrated space where the peculiar intensity distribution of an exotic beam is a point. All variations are measured with respect to that peculiar intensity distribution. Consequently, the above approach can be used to image objects consisting of multiple points using exotic phase masks and faithfully transfer the 3D propagation characteristics to the imaging system.

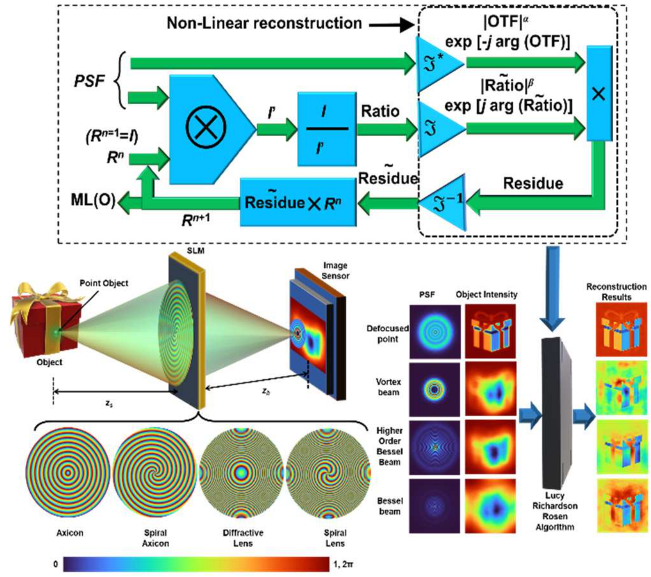

Fig. 1. The optical configuration of indirect imaging using exotic beams and LR^{2}A is shown.

III. SIMULATION

The simulation was carried out with 500 × 500 pixels computational space, with a physical pixel pitch 10 µm, wavelength 650 nm, object to spatial light modulator (SLM) distance z_s = 0.4 m, SLM to sensor distance z_h = 0.4 m, and a diffractive lens with a focal length f set at 0.2 m. To eliminate the direct imaging mode with the diffractive lens, the z_h value was adjusted to 0.2 m. The investigation into 3D imaging encompassed two test objects, object – 1 and object – 2 featuring the letters "CIPHR" and "TARTU." The object intensity pattern I was obtained by a convolution of the object – 1 and object – 2 with PSFs at (z_s = 0.4 m) and PSF (z_s = 0.5 m) respectively followed by an algebraic sum. The PSFs for the above two planes, object intensity distributions and reconstructions using LR^{2}A for a diffractive lens, quasi-random lens, spiral lens with a topological charge of 5 and cubic phase mask are shown in Fig. 2. The cases of the spiral lens, quasi-random lens and diffractive lens have identical axial characteristics, i.e., a high axial resolution. However, for the cubic phase mask, Airy beam is generated which has a low axial resolution or a high focal depth. Therefore, unlike the other cases, with a cubic phase mask, the objects at both planes were reconstructed with the PSF of any of the two planes without any distortion or blur. This demonstrates the faithful transfer of axial characteristics from Airy beam to the imaging system.

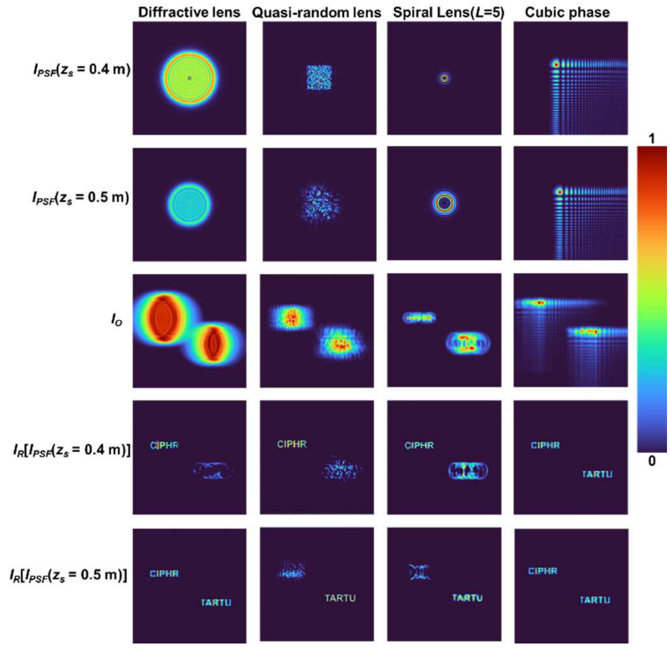

Fig. 2. Simulation results of PSF, object intensity patterns and reconstruction results for the two planes for a diffractive lens, quasi-random lens, spiral lens and cubic phase mask.

IV. EXPERIMENT

In the optical experiment, a high-power LED from Thorlabs (940 mW, λ = 660 nm, and Δλ = 20 nm) was employed using an SLM (1920 × 1200 pixels, pixel pitch 8 µm, Thorlabs Exulus HD2,), and an image sensor (1440 × 1080 pixels with a pixel pitch of ~3.5 µm, Zelux CS165MU/M 1.6 MP). Schematic of the experimental setup is shown in Fig. 3. The light emitted from the object undergoes collimation through a refractive lens with a focal length of 5 cm, then traverses the beam splitter before impinging on the SLM. Phase masks featuring deterministic and random optical fields are displayed on the SLM successively. The image sensor records both the PSF and I. Experimental results of 3D imaging utilizing diffractive lens, quasi-random lens, spiral lens (L = 5), and a cubic phase mask are depicted in Fig. 4. Analysis of Fig. 4 reveals that the axial resolution of the first three elements is high, while the final element exhibits a lower axial resolution.

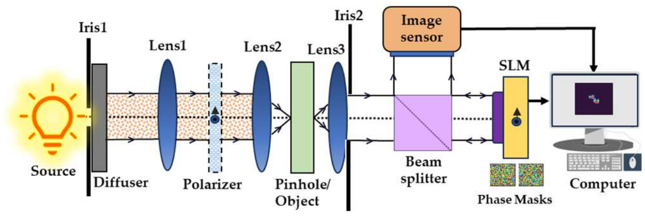

Fig. 3. Schematic of the experimental setup.

A second study with LR^{2}A was carried out using medical images obtained from surgeons. Fig. 5 shows the imaging and reconstruction results of Cone Beam Computed Tomography (CBCT. The patient had multiple jaw implants and metallic artifacts which exhibited blurs. To enhance the image, LR^{2}A was applied with synthetic PSFs. The results obtained from the system and after reconstructing using

LR^{2}A are shown in Fig. 5. A significant improvement in resolution and contrast can be seen.

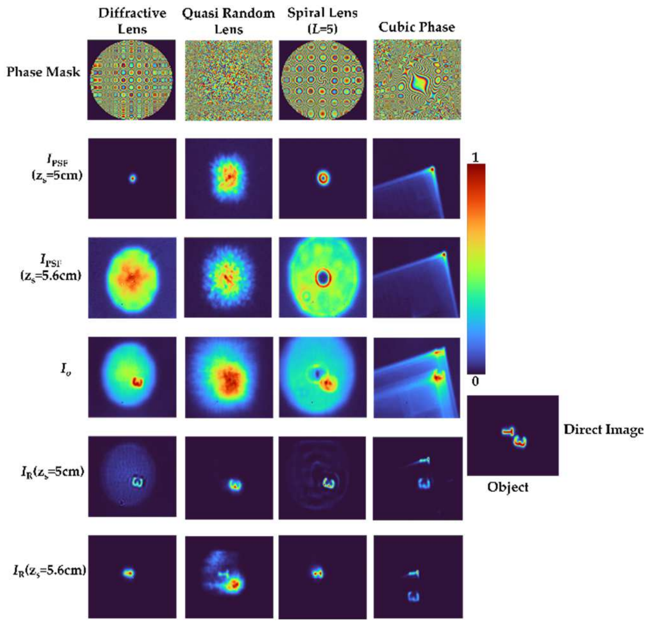

Fig. 4. Experimental results of 3D imaging.

Fig. 6 shows the colonoscopy images captured using an Olympus colonoscope system in conjunction with the Capture ITPro medical imaging software. For this image, the PSF was synthetically created and we extracted different color channels from the images and processed them separately with the synthetic PSF using LR^{2}A. The results obtained from LR^{2}A shows a significant improvement in both contrast and resolution.

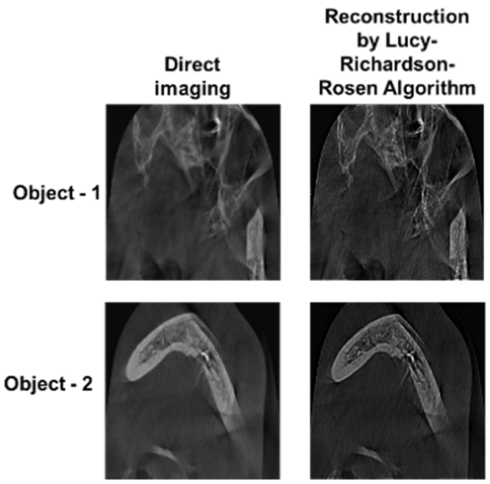

Fig. 5. Experimental results of cone beam computed tomography.

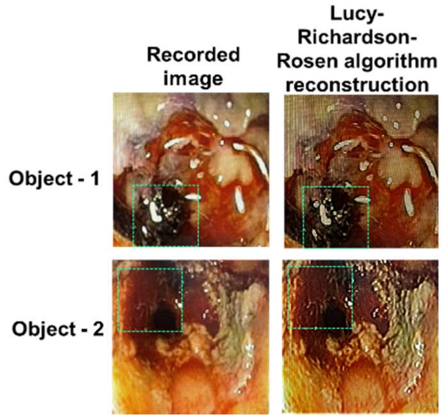

Fig. 6. Experimental colonoscopy results.

V. Summary and Conclusion

The recently developed computational reconstruction method, LR^{2}A, has undergone experimentation involving various deterministic and random optical fields for 3D imaging applications. LR^{2}A demonstrates faithful transfer of axial characteristics from non-imaging beams to the imaging system. Additionally, medical images directly recorded using a colonoscope and cone beam computed tomography (CBCT) were processed using LR^{2}A with synthetic PSFs, resulting in observed enhancements in resolution and contrast. The showcased versatility of LR^{2}A with diverse optical beams is expected to inspire further research, extending LR^{2}A's applicability to coded aperture imaging methods, such as those utilizing ensembles of Airy beams, self-rotating beams, and self-interference holograms for image reconstruction. This study is anticipated to contribute significantly to the future development of advanced coded aperture holography and incoherent digital holography techniques.

Acknowledgment

The authors thank Dr. Scott Clinic, Dr. Jeyasekharan Medical Trust, Rajas Dental College and Hospital and Darshan Dental and Orthodontic Clinic, Kanyakumari, India.

References

[1] F.M. Dickey, “Laser beam shaping: theory and techniques,” *CRC Press,* 2018.

[2] A. P. I. Xavier, F. G. Arockiaraj, S. Gopinath, A.S. J. F. Rajeswary, et.al., “Single-Shot 3D Incoherent Imaging Using Deterministic and Random Optical Fields with Lucy–Richardson–Rosen Algorithm,” *Photonics*, vol. 10, no. 9, pp. 987, Aug. 2023.

[3] R. H. Dicke, “Scatter-Hole Cameras for X-Rays and Gamma Rays”, *The Astrophysical Journal*, vol. 153, pp. L101, Jun. 1968.

[4] J. Rosen, A. Vijayakumar, M. Kumar, M. Rai, R. Kelner, Y. Kashter, A. Bulbul, and S. Mukherjee, “Recent advances in self-interference incoherent digital holography,” *Advances in Optics and Photonics*, vol. 11, no. 1, pp. 1-66, Feb. 2019.

[5] D. Smith et al., “Nonlinear Reconstruction of Images from Patterns Generated by Deterministic or Random Optical Masks—Concepts and Review of Research,” *Journal of Imaging*, vol. 8, no. 6, pp. 174, Jun. 2022.

[6] A. Vijayakumar, M. Han, J. Maksimovic, S. H. Ng, T. Katkus, A. Klein, K. Bambery, M. J. Tobin, J. Vongsvivut, and S. Juodkazis, “Single-shot mid-infrared incoherent holography using Lucy-

Richardson-Rosen algorithm," *Opto-Electronics Science*, vol. 1, no. 3, pp. 210006, Mar. 2022.